Assessing the reliability of peatland GPP measurements by remote sensing: from plot to landscape scale

Assessing the reliability of peatland GPP measurements by remote sensing: from plot to landscape scale.

Kirsten J Lees[1,2]*, Myroslava Khomik[3], Tristan Quaife[4], Joanna M Clark[1], Tim Hill[2], Daniela Klein[5], Jonathan Ritson[6], and Rebekka RE Artz[7]

1. Department of Geography and Environmental Science, University of Reading, Whiteknights, RG6 6DW, UK.
2. Department of Geography, University of Exeter, Streatham Campus, Exeter, EX4 4QE, UK
3. University of Waterloo, ON N2L 3G1, Canada
4. National Centre for Earth Observation, Department of Meteorology, University of Reading, Reading, Whiteknights, RG6 6BB, UK.
5. Forsinard Flows RSPB Office, Forsinard, KW13 6YT, UK
6. Imperial College London, SW7 2A7 UK
7. The James Hutton Institute, Craigiebuckler, Aberdeen, AB15 8QH, UK

Abstract. Estimates of peatland carbon fluxes based on remote sensing data are a useful addition to monitoring methods in these remote and precious ecosystems, but there are questions as to whether large-scale estimates are reliable given the small-scale heterogeneity of many peatlands. Our objective was to consider the reliability of models based on Earth Observations for estimating ecosystem photosynthesis at different scales using the Forsinard Flows RSPB reserve in Northern Scotland as our study site. Three sites across the reserve were monitored during the growing season of 2017. One site is near-natural blanket bog, and the other two are at different stages of the restoration process after removal of commercial conifer forestry. At each site we measured small (flux chamber) and landscape scale (eddy covariance) CO_2 fluxes, small scale spectral data using a handheld spectrometer, and obtained corresponding satellite data from MODIS. The variables influencing GPP at small scale, including microforms and dominant vegetation species, were assessed using exploratory factor analysis. A GPP model using land surface temperature and a measure of greenness from remote sensing data was tested and compared to chamber and eddy covariance CO_2 fluxes; this model returned good results at all scales (Pearson's correlations of 0.57 to 0.71 at small scale, 0.76 to 0.86 at large scale). We found that the effect of microtopography on GPP fluxes at the study sites was spatially and temporally inconsistent, although connected to water content and vegetation species. The GPP fluxes measured using EC were larger than those using chambers at all sites, and the reliability of the TG model at different scales was dependent on the measurement methods used for calibration and validation. This suggests that GPP measurements from remote sensing are robust at all scales, but that the methods used for calibration and validation will impact accuracy.

Keywords: TG model, photosynthesis, NDVI, satellite, blanket bog

*Corresponding author: K.lees@exeter.ac.uk

1 Introduction

Peatlands are important ecosystems for carbon sequestration, but many areas in the Northern Hemisphere have experienced degradation through human land use. As an organic-rich, water-saturated substrate, peat stores huge amounts of carbon relative to the land area it occupies due to inhibited decomposition. In Scotland, peatlands store 56% of total soil carbon whilst occupying 24% of the land area (Chapman *et al.*, 2009). Many peatland areas have, however, been subject to managements such as draining, grazing, burning and planting for commercial

forestry, which have reduced saturation and increased bulk density of the peat (JNCC, 2011). Restoration of peatland areas is of interest to policy makers as a carbon emissions abatement scheme (IUCN, 2016; European Commission, 2018), but needs to be based on a robust understanding of peatland ecosystems in order to effectively reverse previous damage. Practitioners need techniques to assess changes in peatland carbon fluxes at a landscape scale in order to measure the success of restoration processes and detect where to focus further efforts.

Upscaling of ecosystem processes is an important research area in ecology, as landscape and regional scale estimates are needed for policy decisions and carbon accounting (Fu *et al.*, 2014; Le Clec'h *et al.*, 2018). Blanket bogs (peatland covering large areas and sustained by rainfall and relatively low annual temperature fluctuations (Lindsay, 2010)) in particular have small-scale heterogeneity in topographic features known as hummocks and hollows, which can vary at scales of less than a metre (Belyea and Clymo, 2001). This microtopographical variation influences vegetation communities, which can induce significant variation in carbon fluxes (Dinsmore *et al.*, 2009; Arroyo-Mora *et al.*, 2018; Peichl *et al.*, 2018).

Conventional methods of carbon dioxide (CO_2) exchange measurement include flux chambers and Eddy Covariance (EC) towers, both of which cover relatively small areas and are expensive to manage and maintain. Remote sensing has the potential to help monitor carbon fluxes in these important, remote and extensive areas that are difficult to access for conventional field-based measurements as well as sensitive to trampling, yet little testing of methods has been carried out (Lees *et al.*, 2018). The existence of satellites with very fine spatial resolution (to tens of metres in freely accessible data) means that studies can now consider variation within a landscape, but the microtopography of blanket bogs is still at a scale that is too fine to be detectable from non-commercial satellite data (Becker *et al.*, 2008). Models using satellite data to estimate carbon fluxes are being developed to cover large areas (Lees *et al.*, 2018) and have

recently shown successes in estimating carbon fluxes from peatland landscapes (Kross, Seaquist and Roulet, 2016; Lees, Quaife, *et al.*, 2019), but there is still uncertainty over whether these models can adequately detect the variation from small-scale peatland heterogeneity (Zhang *et al.*, 2007; Arroyo-Mora *et al.*, 2018). The focus of this study is therefore to assess whether the small-scale variations in carbon fluxes due to microtopography can be detected using remote sensing data, and whether large scale estimates using these techniques are a reliable estimate of the average fluxes resulting from these mosaic landscapes.

A Temperature and Greenness (TG) model is specifically considered in this study, as this has previously been shown to give good agreement with EC data over the same study area as used in this work (Lees, Quaife, *et al.*, 2019). This model combines a measure of land surface temperature with a vegetation index, in this case the Normalised Difference Vegetation Index (NDVI), to give an estimate of Gross Primary Productivity (GPP).

The aim of this work is to consider what factors affect GPP in blanket bog, and whether the results from large scale models using satellite data can give reliable estimates of photosynthesis measurements made at smaller scales. We hypothesise that the TG model will give good agreement with chamber flux data at the small scale, and with EC data at the larger scale. We also expect that the measurements and estimates at different spatial scales will show similar results in both patterns and values. The approaches are tested at the Forsinard Flows RSPB (Royal Society for the Protection of Birds) reserve, which is an ideal study location as it has a chronosequence of areas undergoing restoration from commercial forestry (Hancock *et al.*, 2018), and long-term Eddy Covariance (EC) monitoring of greenhouse gas emissions (Hambley *et al.*, 2019) at several of the restoration sites.

2 Methods

2.1. Field sites

This research is based at three field sites within the Forsinard Flows RSPB reserve in Northern Scotland (approx. 58.36, -4.04 to 58.43, -3.63, WGS84). The reserve is part of the much larger blanket bog Flow Country EU Natura site. Cross Lochs is a near natural site (see Levy and Gray, (2015), where no drainage has been applied. An EC tower is located at 58.3703,-3.9644 (WGS84), elevation 211 m.

Talaheel and Lonielist are both sites undergoing restoration, which were previously drained and subsequently planted for commercial conifer (sitka spruce *Picea sitchensis* and lodgepole pine *Pinus contorta*) forestry in the mid to late 1980s.

Talaheel was initially felled in 1998, with the trees laid into the planting furrows; some areas have since undergone partial further landscaping (which affects half the points in this study) to crush the decomposing conifer brash and to create peat dams in the furrows (winter 2015/16). This has led to raised water levels across the site (see Hancock et al., 2018). The EC tower is located at 58.4146, -3.8006 (WGS84), elevation 196 m.

The conifer plantation at Lonielist was felled in winter 2003/2004. At the time of measurement, it retained the distinctive pattern of ridges on which the trees were planted, and drainage ditches infilled with the felled trees. This site had undergone no further management until the end of this project (-end of 2017). The EC tower is located at 58.3910, -3.7651 (WGS84), elevation 180 m.

All three sites are subject to some light grazing by wild red deer (*Cervus elephantus*). Talaheel is fenced as part of a larger enclosure including some forestry, although some deer are present inside the fence, whilst Lonielist and Cross Lochs are entirely open to grazing.

Small scale measurement points were set up in the area within each site's EC tower footprint. The precise distances from the tower and dominant wind directions (Northwest and Southwest) were determined from Hambley (2016) to incorporate appropriate locations within the average

flux tower footprints. At each site two perpendicular crossing transects were set up, one including five points and extending away from the tower into the dominant wind direction, and one including four points and extending into the secondary wind direction (see Figure 1). At Lonielist the main transect was 80 m and the secondary transect was 60 m, with all points 20 m apart. At Talaheel the transects were 100 m and 75 m with the points 25 m apart, and at Cross Lochs the transects were 120 m and 90 m with points 30 m apart. At each point two PVC collars (24 cm in diameter) were placed: one on higher microforms (ridges in the restored sites, hummocks at Cross Lochs) and one on lower microforms (in the furrows at the restored sites, hollows at Cross Lochs); therefore, there were 16 collars at each of the three sites. The collars were 8 cm depth and were inserted to approximately 4 cm below ground. At least 24 hours were allowed between collar insertion and first measurements.

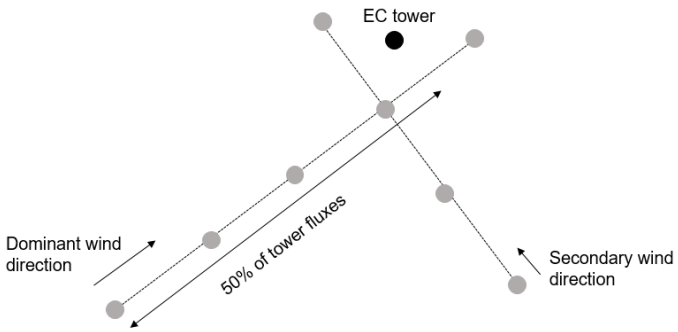

Figure 1 – Location of points within the tower footprint. Two collars, one on a higher microform and one in a lower area, were placed at each point.

2.2. Chamber flux measurements

Monthly in situ CO_2 flux measurements beginning March and ending September 2017 were taken using a LICOR-8100A (LICOR Inc., Lincoln, Nebraska, USA) portable infrared gas analyser and custom Perspex chambers of 24 cm diameter and 30 cm height. Small 9V battery-operated fans were installed within the chambers to circulate the air. The two chambers, one clear and one covered with a blackout cloth, were sealed to the collars using rubber mastic

(Terostat), and consecutive measurements were taken with a brief aeration period as the chambers were exchanged. Each measurement period was five minutes, with a 20 second pre-measurement stabilisation period. Chamber flux measurements were usually taken between 8 am and 2 pm, although this was sometimes altered due to weather conditions. Each collar was measured once with a clear-chamber and once with a blackout chamber on each visit except when adverse weather conditions prevented a full dataset being collected.

2.3. Field spectrometry

Spectral measurements in the field were taken on the same visits as the chamber flux data collection using a handheld SVC HR-1024 (Spectra Vista Corporation, spectral resolution 3.5 to 9.5 nm) spectroradiometer mounted on a monopod and held approximately 1m from the surface using an 8˚ FOV lens with an on-the-ground footprint within the diameter of the collars. The spectral range of the instrument is from 337 nm to 2521 nm. Three measurements were taken of the vegetation within each collar, at three different angles to minimise structural effects (opposite the position of the sun and at 90˚ to either side). A Spectralon reference panel was also measured before each observation (within a minute) to normalise from radiance to reflectance.

The Normalised Difference Vegetation Index (NDVI) is calculated from the difference between reflectance in red wavelengths of light, which plants absorb strongly, and the near-infrared (NIR), which plants reflect:

$$NDVI = (R_{NIR} - R_{red})/(R_{NIR} + R_{red}) \quad (1)$$

In this study we calculated the red and NIR bands as the average of the values in wavelengths 630-680 nm and 845-885 nm respectively.

2.4. Other factors measured in the field

Photosynthetically Active Radiation (PAR) was measured outside the chamber during clear chamber measurements. Soil moisture was measured using a moisture probe with 6 cm prongs (Theta probe ML2x connected to HH2 moisture meter, Delta-T Devices). At the Lonielist site, dipwells were inserted within a metre of each collar, and the water level was monitored manually at the same time as the spectral measurements were taken. A lollipop thermometer (Fisherbrand, accurate to ± 1˚C) was used to measure soil temperature outside the collar at two different depths, 5 cm and 15 cm. The thermometer was also used to measure temperature within the vegetation inside the chamber at the start and end of each flux measurement. These measurements were taken on the same dates and at the same plots as other monitoring (above).

To consider the different vegetation communities of the microforms, the species within the collars were surveyed in June 2017. All species were recorded as percentage cover over the area of the collar, and overlapping canopies sometimes allowed total percentage cover to be over 100%. Six species which were found at all three sites were selected as indicators of microform vegetation communities. These are shown in Table I.

Table I – species selected which were present at all three sites, which microform they prefer, and their average (and standard deviation) percentage coverage in collars at each site.

Common name	**Latin name**	**Hummock or Hollow**	**Lonielist**	**Talaheel**	**Cross Lochs**
Heather	*Calluna vulgaris*	Hummock	7.5 ± 11.7 %	4.7 ± 9.8 %	9.7 ± 9.5 %
Common cotton grass	*Eriophorum angustifolium*	Hollow	10.9 ± 13.6 %	17.9 ± 15 %	9.4 ± 10.5 %
Reindeer lichen	*Cladonia portentosa*	Hummock	12.8 ± 18 %	17.6 ± 26.9 %	11.4 ± 18.2 %
Red bogmoss	*Sphagnum capillifolium*	Hummock	19.9 ± 22.5 %	16.7 ± 30.1 %	27.7 ± 18.1 %
Red-stemmed feather moss	*Pleurozium schreberi*	Hollow	12.3 ± 22.1 %	23.6 ± 27.9 %	3.9 ± 7.2 %

Deer grass	*Trichiophorum germanicum*	Hollow	0.6 ± 2.5 %	4.9 ± 8.3 %	21.8 ± 21.6 %

179

180 *2.5. Eddy Covariance*

181 Eddy covariance data from the whole of 2017 was used, except for Lonielist where data
182 collection began on the 24th of March.

183 Net ecosystem exchange of CO_2 (NEE) at Lonielist was measured using a LI-7200 enclosed
184 CO_2/H_2O infrared gas analyser (LI-COR Biosciences Inc. Lincoln, NE, USA), and a Gill HS-
185 50 3-D sonic anemometer (Gill Instruments, Lymington, UK). Data was collected at 20Hz
186 frequency and recorded every half-hour onto a 16GB USB by the LI-7550 Analyzer Interface
187 Unit (LICOR Biosciences, Inc. NE, USA). An insulated 1-meter intake tube was used and the
188 flow was controlled by the Flow Module (7200-101, Li-Cor Inc., Nebraska, USA) to be about
189 15L/min. The instruments were mounted on top of a scaffolding-tower at 2.90 m height,
190 pointing into the predominant wind direction (W-SW, 240˚ North offset).

191 At Talaheel, NEE was measured using the LI-7500A open path CO_2/H_2O gas analyser (LI-
192 COR Biosciences Inc. Lincoln, NE, USA) with a custom enclosure added to the analyser to
193 create an enclosed system (Clement *et al.*, 2009), and a CSAT sonic anemometer (Campbell
194 Scientific, Logan, USA) (Hambley *et al.*, 2019). Data was measured at 10Hz frequency and
195 recorded every half-hour on a flash-card by the CR5000 datalogger. Instruments were set-up
196 at 4.3 m height on a scaffolding tower.

197 At Cross Lochs NEE was measured by the IRGASON - an open-path infra-red gas analyser
198 integrated into a 3D-CSAT anemometer, and controlled by the EC100 electronics control
199 module (Campbell Scientific Ltd. UK). Data was measured at 10Hz, processed by the onboard
200 EasyFluxDL software (Campbell Scientific Ltd. UK) into half-hourly corrected and averaged
201 fluxes and recorded on a flashcard by the CR3000 datalogger. EasyFluxDL software processes

the EC data using commonly used corrections in the scientific literature (Campbell Scientific, 2016). The instruments were set up at 2.3 m height on a tri-pod tower, pointing 310^{o} NW in the predominant wind direction.

The flux data collected by the EC systems at Lonielist and Talaheel were processed using the EddyPro® software (v7.0.4, Li-Cor Inc, Nebraska, USA), in Express mode, on a PC in the office. Similar to EasyFluxDL, EddyPro® uses the most accepted and cited techniques in scientific literature to compute fully-processed half-hourly fluxes. For more details on EddyPro®, please see the EddyPro® manual (LI-COR Biosciences, 2017) and Fratini and Mauder (2014). The processed half-hourly NEE fluxes from all three sites were further processed in a custom R-software script (R Core Team, 2018) to quality check the data – making sure that each half hour had at least 80% of records, that each half hour NEE value was within 3.5 standard deviations of the running 10-hour means and that the data was within physically plausible values for each ecosystem. Using R-code adapted from "http://footprint.kljun.net/download.php" [November 2018]), a flux footprint analysis was performed following Kljun *et al.* (2015) to ensure that all fluxes originated from within 80% of the area of interest. Footprint filtered NEE fluxes were gap-filled and partitioned into GPP and Re, following the methods and code (REddyProc, R-script) of Wutzler *et al.* (2018). This script also estimated the u-star threshold for the data, which was used to further filter out data during times of low turbulence, before partitioning and gap-filling.

Measurements at Lonielist began in March, so 23% of the data was missing at the start of the 2017 year. 26% of available (13550 hh) NEE half-hours were gap-filled at Lonielist, 52% at Talaheel (of 17520 hh), and 60% at Cross Lochs (of 17520hh).

For comparison with the chamber and spectrometer data (TG1, see Section 2.7), the EC half-hourly data covering the same time periods as the chamber flux measurements were used, doubled to give an hourly timestep. For comparison with the TG model using MODIS data

(TG2, see Section 2.7), the EC fluxes were averaged across 8-day periods and then multiplied to give daily values, following Lees, Quaife, *et al.* (2019).

2.6. Satellite data

The Moderate Resolution Imaging Spectroradiometer (MODIS) on satellite Terra was used in this study as an example of a medium resolution broad band satellite, which is widely used in environmental studies. Pixels containing the EC towers were downloaded for this analysis. Two MODIS products were used in this study, the 250 m MOD13Q1 NDVI product (Didan, 2015), and the 1 km MOD11A2 Daytime Land Surface Temperature (LST) product (Wan, Hook and Hulley, 2015). The NDVI product is given in 16-day periods, whilst the LST product is given in 8-day periods. The MODIS data products were downloaded using the MODIS ORNL web service through Matlab code (Santhana Vannan *et al.*, 2009). Cloud filtering was applied to remove pixels extensively affected by cloud cover, whilst letting through data which was affected by clouds but still useable (Lees, Quaife, *et al.*, 2019). Each of the MODIS products contains information about the quality of the data in each pixel, and this was used to select which 8-day or 16-day pixels were useable. MOD13Q1 pixel reliability index was used to remove snow/ice or cloud affected values, whilst allowing marginal data. MOD11A2 quality control data was used to remove periods when data was not produced due to cloud effects or other issues. 17-50% of the data at each site were excluded following this protocol. Gap-filling was then performed across each year using the techniques described by Wang et al. (2012), before combining the data into the TG model.

2.7. The TG model

The Temperature and Greenness (TG) model combines a measure of temperature with a vegetation index to give an estimate of GPP (Sims *et al.*, 2008). The model is formulated

following Moore et al. (2013), but using NDVI following the results of Lees, Quaife, *et al.* (2019):

$$GPP = NDVIs \times LSTs \times m \quad (2)$$

$$NDVIs = NDVI - 0.1 \quad (3)$$

$$LSTs = \min[(LST-minLST)/(optLST-minLST), (maxLST-LST)/(maxLST-optLST)] \quad (4)$$

Where NDVIs is the scaled Normalised Difference Vegetation Index and LSTs is the scaled Land Surface Temperature (see Sims *et al.,* 2008; Lees, Quaife, *et al.,* 2019). The scaled NDVI removes low values of NDVI which show no GPP. minLST, optLST and maxLST (given in ˚C) are the minimum, optimum and maximum Land Suface Temperature calculated for a specific ecosystem. We have used 40˚C, 25˚C and -2.5˚C for maxLST, optLST and minLST respectively, following Lees, Quaife, *et al.*'s (2019) work on the same study sites. Furthermore, 'm' is a site-optimisation parameter, and the GRG Nonlinear Solver in Microsoft Office Excel 2013 was used to optimise this parameter at both small and large scales (see Section 4 for discussion of calibration).

Three different formulations of the TG model are used in this study to assess the effect of scale versus methodological bias. These versions are:

TG1 - Small-scale TG model using spectrometer data

The 'm' parameter for the TG model using spectrometer data was optimised to the chamber data across all months and sites and was given the value 0.4397. This small-scale version of the TG model gives an estimate of GPP per hour.

TG2 - Large-scale TG model using MODIS data

The 'm' parameter for the TG model using MODIS data was optimised to the EC data across the whole of 2017 (where EC data was available) and across all three sites. It was given the value 8.046. This large-scale version of the TG model gives an estimate of GPP per day.

TG3 – Small-scale TG model using MODIS data

The small-scale 'm' parameter was applied to the large-scale TG model to give an hourly estimate of GPP using MODIS data.

2.8. Statistical analysis

An Exploratory Factor Analysis (EFA) was used to simplify the large range of variables measured which could affect GPP on a small scale. EFA is a variable reduction technique designed to draw out the underlying factors affecting the measured variables. In this case the EFA was used because we expected that the variables measured were related to each other by means of underlying constructs, for example, the presence of certain vegetation species was likely to be correlated due to underlying features of their microhabitats.

The variables considered included those explained in Section 2.4 (selected vegetation species, PAR, surface temperature, soil temperature at 5 cm and 15 cm, soil moisture, and microforms), and also the NDVI, which is a measure of vegetation greenness and health, and the Normalised Difference Water Index (NDWI, using NIR and Short-Wave Infrared (SWIR)) which has been shown to have a relationship with moisture conditions in peatland vegetation (Lees *et al.*, 2019). Repeated measures were accounted for by including the time of year as a variable; in order to create a linear relationship, daylight period was used as a measure of season. These variables are referred to in the results by short names given in Table II.

TableII –Variables used in the EFA, and what they refer to.

Short name	**Description**
Feather_moss	The proportion of *P schreberi* in the collar (%)

Reindeer_lichen	The proportion of *C portentosa* in the collar (%)
S_cap	The proportion of *S capillifolium* in the collar (%)
Deer_grass	The proportion of *T germanicum* in the collar (%)
Cotton_grass	The proportion of *E angustifolium* in the collar (%)
Heather	The proportion of *C vulgaris* in the collar (%)
NDWI	The calculated NDWI of the collar from the hand-held spectrometer
NDVI	The calculated NDVI of the collar from the hand-held spectrometer
PAR	The average PAR across the clear chamber flux measurement period.
Surface_temp	The temperature amongst the vegetation at the soil surface (˚C)
Soil_temp_5cm	The soil temperature at 5 cm depth (˚C)
Soil_temp_15cm	The soil temperature at 15 cm depth (˚C)
Light_period	Daylight period of the day of measurement in Scotland
microfeature	Whether the collar was on a high area (hummock/ridge) or low area (hollow/ditch)

The EFA was limited to five factors after initial statistical exploration of different numbers of factors suggested that this was the best option for all three sites; we found that using five factors explained the majority of the variance seen in variables at each site (see supplementary material). The resulting factor scores were correlated with the GPP in order to assess which factors and variables were most important in determining peatland GPP at small scales, and whether these could be assessed using remote sensing.

All analysis was done in base R (R Core Team, 2017). All results collected specifically for this study are available online (Lees, Clark, *et al.*, 2019).

3 Results

3.1. Factors affecting GPP at small scale

The six vegetation species considered in this analysis show several significant differences between hummock and hollow percentage coverage (see Figure 2). At the near-natural Cross Lochs (Figure 2C) site there is significantly more heather (*C vulgaris*) and *S capillifolium* on

307 the hummocks, but significantly more deer grass (*T germanicum*) in the hollows. The Lonielist
308 site (Figure 2A) also has significantly more heather on the hummocks, but significantly more
309 red-stemmed feather moss (*P schreberi*) in the hollows. There were no significant differences
310 between hummock and hollow vegetation at the Talaheel site in 2017 (Figure 2B).

311 There are also differences between the three sites in terms of vegetation cover. Cross Lochs is
312 richer in deer grass than the other two sites, whilst Talaheel has higher cover of common cotton
313 grass (*E angustifolium*). The intact site Cross Lochs also has a greater variety of species, with
314 some present that were not included in our collars at the other two sites such as bog myrtle
315 (*Myrica gale*), bog asphodel (*Narthecium ossifragum*), and sundew (*Drosera rotundifolia*).

A - Lonielist

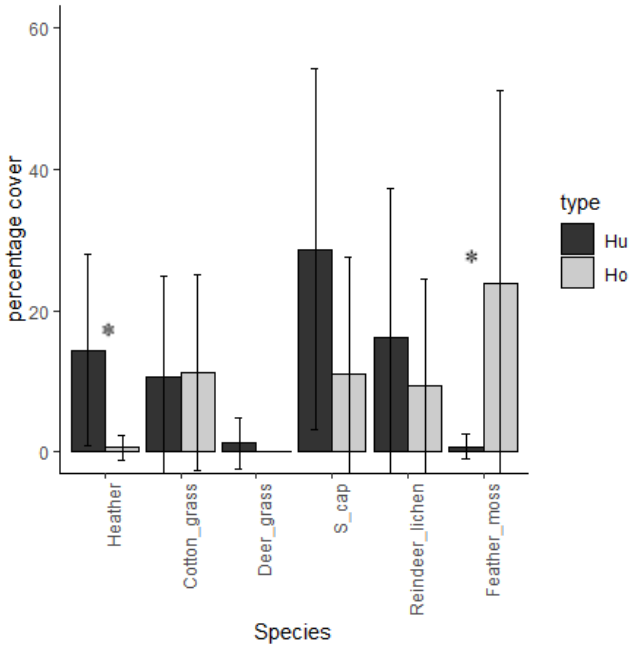

316

B - Talaheel

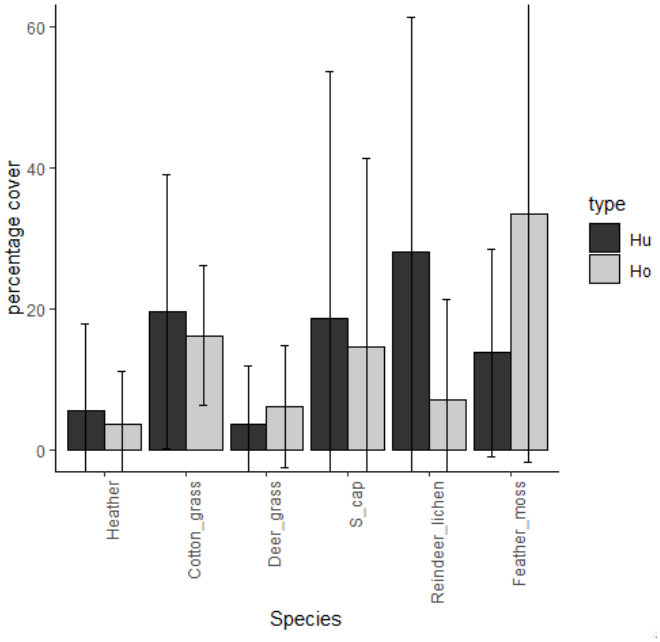

317

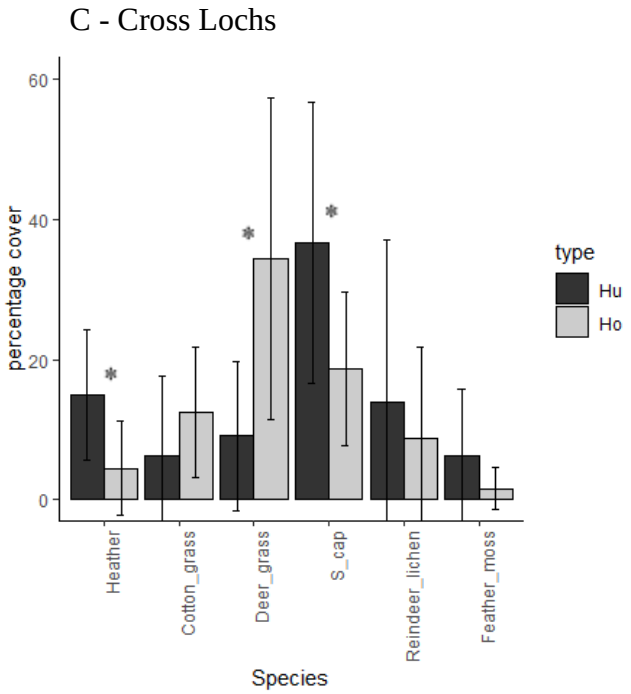

Figure 2 –Species differences between hummocks and hollows at the three sites (A: Lonielist, B: Talaheel, C: Cross Lochs). Stars show significant difference between hummock and hollow (n=8, $p<0.05$).

These selected vegetation species were also used in the EFA, where they are linked to underlying factors which also affect microtopography (all sites), the NDWI (Talaheel and Cross Lochs), and soil moisture (Cross Lochs). These factors also correlate with GPP.

The EFA results are shown in Figure 3, along with the factor Pearson's correlations with GPP. At Lonielist (Figure 3A) the second factor has the highest correlation with GPP (0.68) and is linked with the NDVI and the three temperature variables. The third and fourth factors also show some correlation with GPP (0.21, 0.28) and are connected with the microforms variable and the vegetation species variables.

At Talaheel (Figure 3B) the first and third factors show correlations with GPP (0.45, 0.25). The first factor is connected to the NDVI, NDWI, and temperature variables, whilst the third is linked with the NDWI and NDVI, and percentage cover of *S. capillifolium*, reindeer lichen, and feather moss.

At Cross Lochs the first factor is correlated with GPP (0.49) and links with light period, temperature, NDWI and PAR. The second factor also correlates with GPP (-0.22) and is connected to the microform variable, several plant species, soil moisture and the NDWI. The negative correlation here suggests that the collars classed as hollows have a higher GPP than those classed as hummocks; this is opposite of the result at Lonielist. The third factor correlates positively with GPP (0.38) and is connected to the two soil temperature variables, NDWI and NDVI.

A - Lonielist

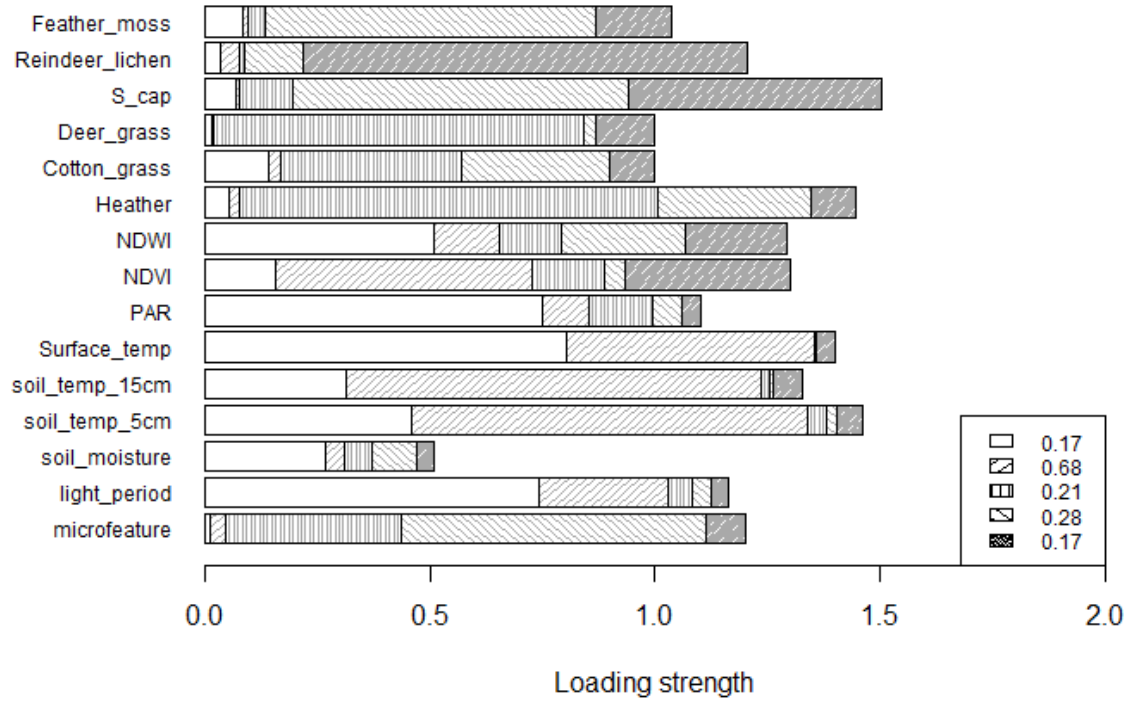

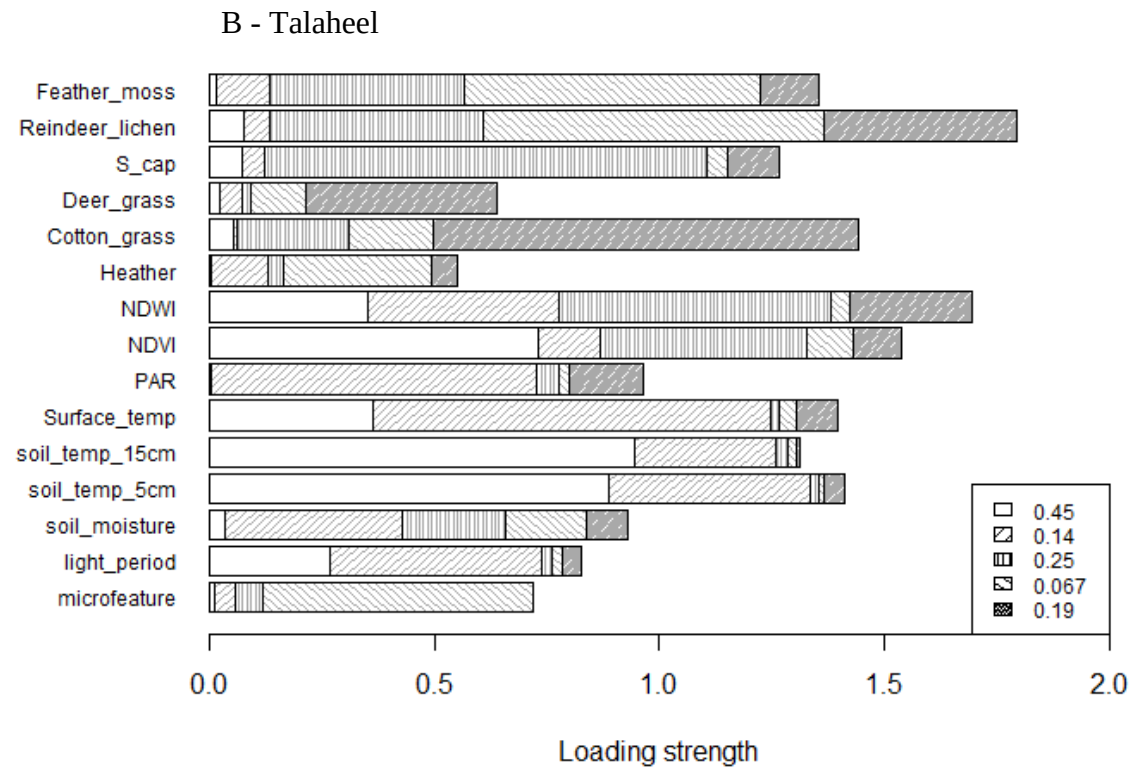

342

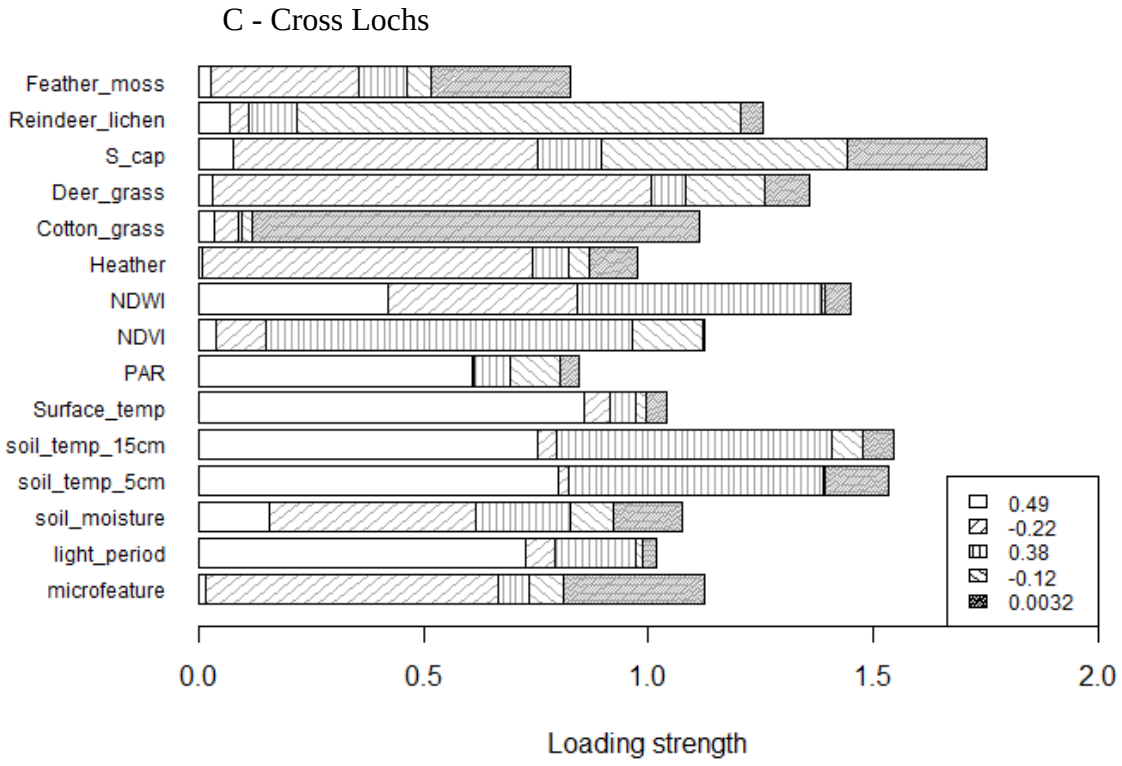

343

344 **Figure 3** – Lonielist, Talaheel and Cross Lochs factors. Each of the five factors is indicated by a different
345 pattern fill. The variables are given on the y axis, and the factors which underly and are connected with each
346 variable have a loading strength shown by the stacked bar lengths. Legends show correlation of the scores for
347 each factor with GPP values. For example, the first factor at Cross Lochs is shown by the white bars, and has

high loading strengths associated with PAR, the three temperature variables, and the light period. It also has a correlation of 0.49 with GPP. See supplementary material for more information.

3.2. Comparison of modelled and measured GPP at small scale

Figure 4 shows the TG model using the spectrometer NDVI and the surface temperature applied to each of the sites across the measurement period, with the 'm' parameter calibrated to the chamber data (TG1). The agreement between the model and the chamber data is very good temporally, with the boxplots well within error bars across the year. The chamber fluxes have larger ranges than the TG model results at each site throughout the growing season. The TG model tends to underestimate the highest chamber GPP values, as can be seen from the scatter plots in Figure 4.

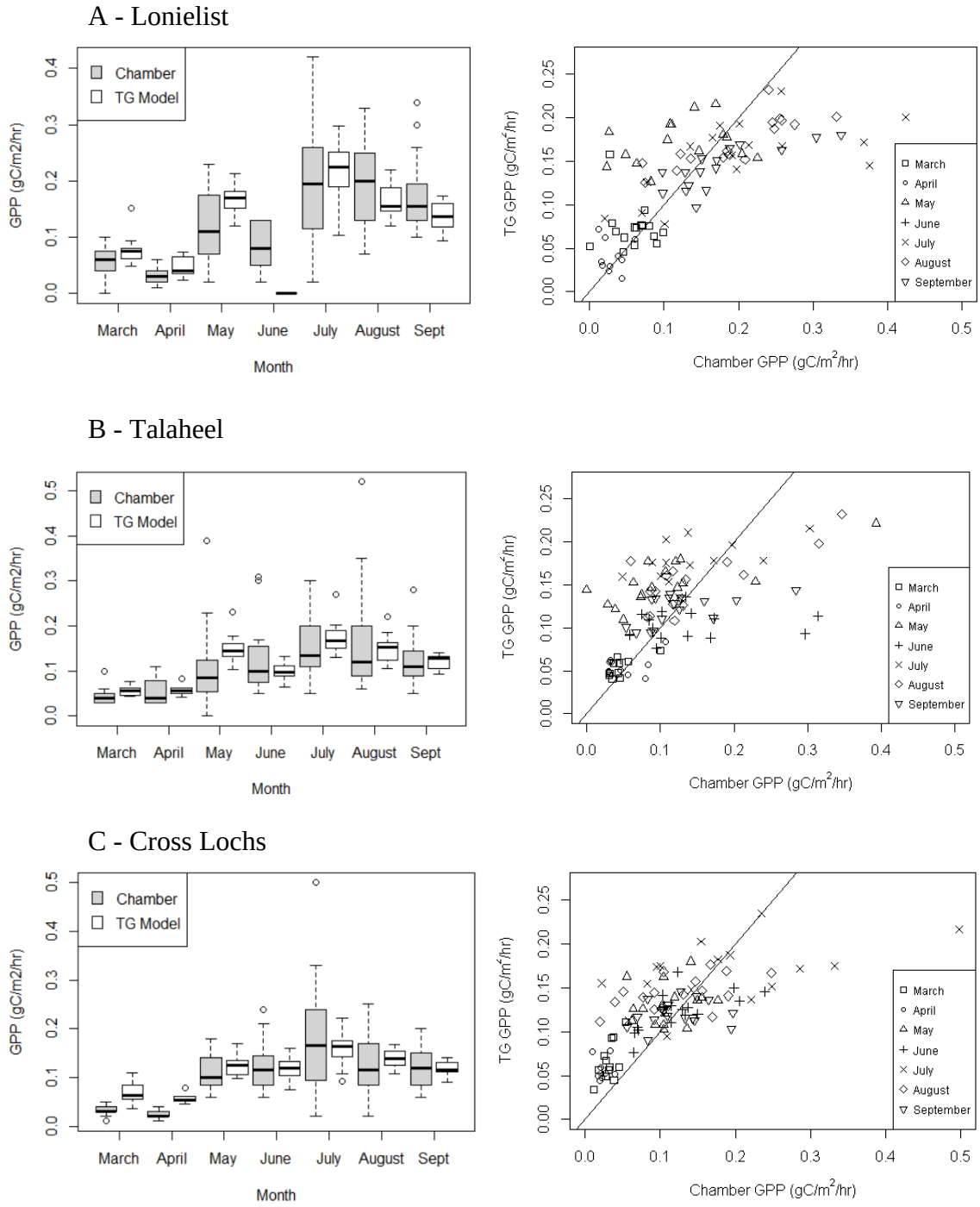

Figure 4 - Boxplots and scatterplots (by month) comparing the chamber-measured GPP and GPP calculated from the TG model using hand-held spectrometer data and the surface temperature measurements for each site (TG1). There is no TG model result in June at Lonielist due to the poor weather causing lack of spectral measurement. 1:1 lines are plotted on the scatter graphs.

3.3. Comparison of small-scale modelled and measured GPP with EC and satellite data

Figure 5 shows the average GPP across the experiment period from the chamber data and EC data, and modelled from the spectrometer (TG1) and MODIS (TG2 and TG3) data. The Pearson's correlations between the chamber fluxes and the spectrometer TG1 fluxes across all months are 0.57 ($p<0.01$, $n=98$) at Talaheel, 0.71 ($p<0.01$, $n=89$) at Lonielist, and 0.70 ($p<0.01$, $n=101$) at Cross Lochs. TG2 using MODIS data is calibrated on a daily rather than hourly time frame, and the Pearson's correlations between the EC data and the MODIS TG2 model (DoY 70 to 265) are 0.76 ($p<0.01$, $n=23$) at Lonielist, 0.76 ($p<0.01$, $n=24$) at Cross Lochs, and 0.86 ($p<0.01$, $n=24$) at Talaheel.

The chamber GPP is lower than the time-period-matched EC GPP at all three sites (54.9% lower at Lonielist, 72% at Talaheel, 62% at CrossLochs). The TG3 model using MODIS data and the 'm' parameter calibrated from small-scale data matches better with hourly chamber fluxes than EC fluxes.

The difference between chamber GPP from hummocks and hollows is greatest at Lonielist and shows higher GPP values from hummocks. The difference is less pronounced at Cross Lochs, but shows the opposite effect, with higher GPP from hollows. Talaheel shows less clear differences between the two types of microform. At all three sites the differences in microtopography shown by the spectrometer TG results are less pronounced than those from the chambers. As the differences between GPP from hummocks and hollows are small and inconsistent, area-weighting was not used in upscaling estimates for this study.

A – Lonielist

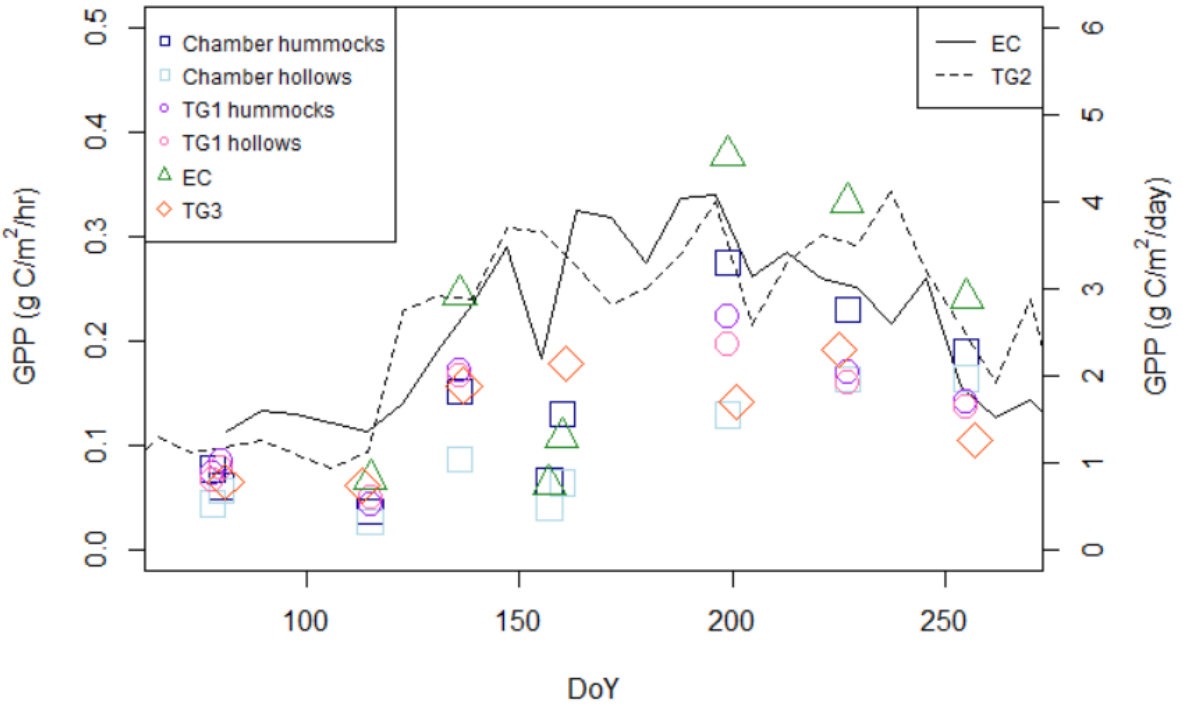

385

B - Talaheel

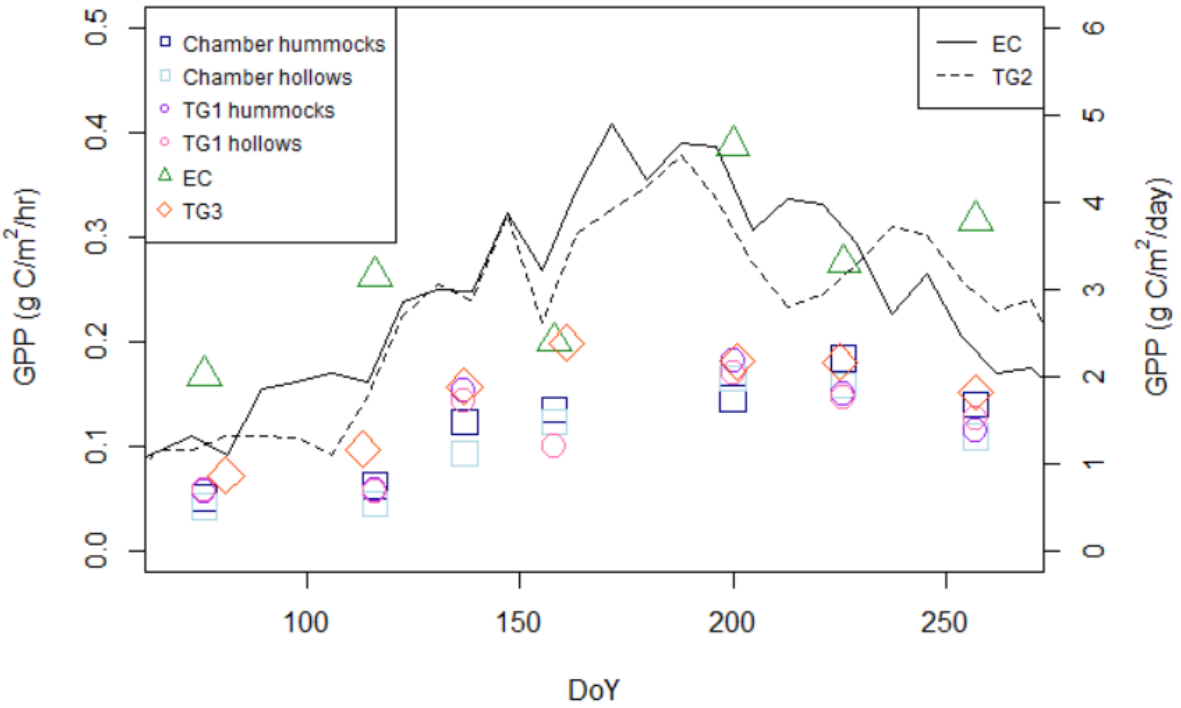

386

387

388

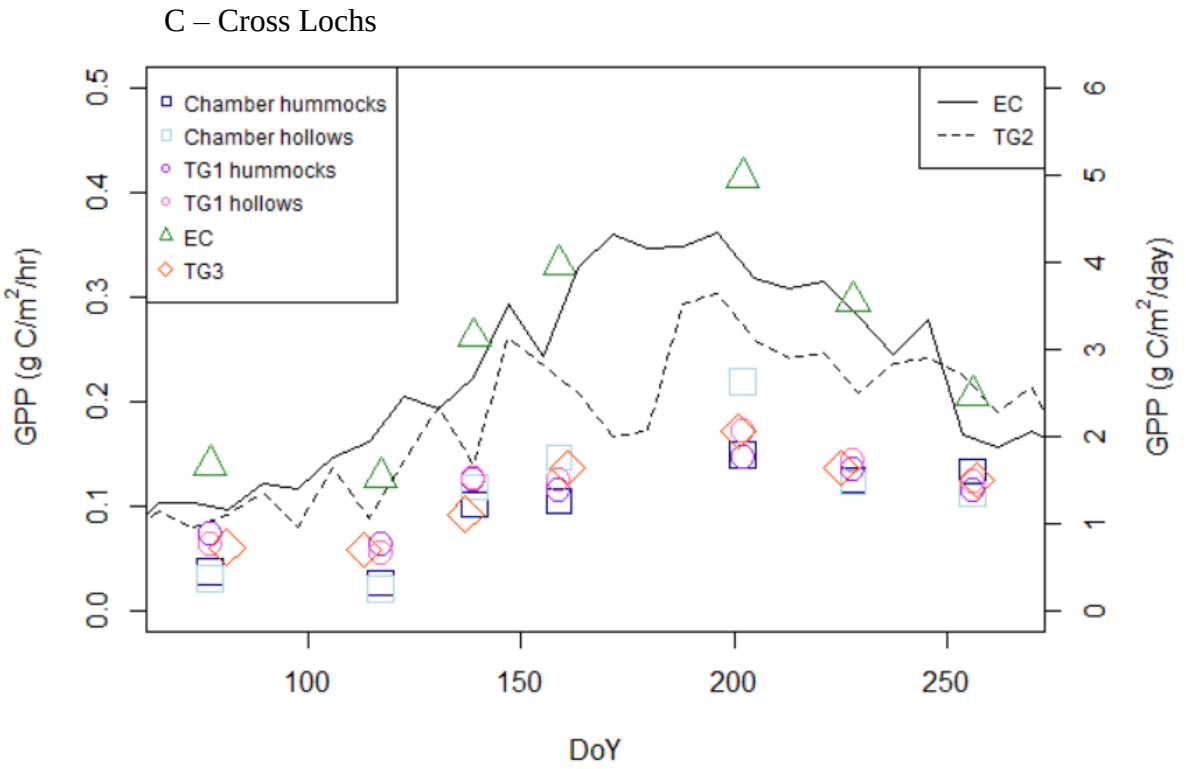

389

390 **Figure 5** – The different estimates of GPP for each site across the growing season. The results represented by
391 coloured symbols and the left-hand axes show the measurements and model results that are calibrated to an
392 hourly timestep and only calculated during manual field measurement periods. These include the flux chamber
393 data from hummocks and hollows, the TG1 model results for hummocks and hollows, the EC data averaged
394 across the half-hourly periods covering the chamber flux measurement period, and the TG3 model. The results
395 represented by the black lines and the right-hand axes show the measurements and model results that are
396 calibrated to a daily timestep and are continuous across the growing season of 2017 due to automated measuring
397 systems. These include the EC data averaged over 8-day periods, and the TG2 model.

398

399

4 Discussion

The EFA correlations with GPP showed that the NDVI and temperature were dominant in the factors affecting GPP at all sites. This endorses the use of the TG model, which makes use of both these variables. All three temperature variables, at surface, 5 cm and 15 cm, were included as variables, but they are strongly related and only one is necessary in the model. The surface temperature provides much more short-term variation compared to soil temperature, and has a relationship with the incoming radiation available for photosynthesis, as shown by the EFA. The variation which surface temperature adds to the model is therefore more than seasonal change, and can provide information on day-to-day changes in GPP due to weather and radiation, and even changes throughout the day.

Lonielist GPP results at small scale showed the greatest difference between hummocks and hollows, particularly in July when we had clear skies and high temperatures during the measurement period. This difference may be more evident at Lonielist than the other sites due to the relic furrow and ridge system creating more extreme microtopographical features than would otherwise be found in a blanket bog. Wu et al. (2011) found that there was no difference in simulated GPP using the McGill Wetland Model between hummocks and hollows at the Mer Bleue bog in Canada, consistent with our results from Talaheel, but did find a significant difference in respiration with hummock ecosystem respiration higher than hollows. They showed that shrubs were the dominant influence on hummock carbon cycling, whilst mosses were the dominant factor in hollows. In contrast, Waddington and Roulet (1996) used flux chamber measurements to show that hummocks at their study site in a Swedish peatland had greater CO_2 uptake than hollows during the growing season, similar to our results at Lonielist. It is somewhat surprising that Cross Lochs, the near-natural site, showed a small but opposite difference in fluxes between microforms.

Lindsay et al. (1988) found that some areas of the Flow Country were dominated by pool and hollow type landforms due to the wet climate, and it may be the case that our classifications of landforms at Cross Lochs were based on the need to distinguish areas of different heights within close range, and did not always satisfy the descriptions of true hummocks and hollows. In general, the differences in GPP fluxes between microforms did not seem to be large or temporally consistent during our study period. The period during which measurements were taken was generally quite wet, with June, July and August all having higher rainfall totals than the 1981-2010 average (Met Office, 2012, 2018). A stronger difference between fluxes from microforms might have been seen under dryer conditions. This is corroborated by previous studies that have found significant differences between carbon fluxes from different microforms linked to soil moisture (Heikkinen *et al.*, 2002; Laine *et al.*, 2006). Despite small differences in GPP among the chamber locations, we did observe significant differences in vegetation between the microtopographical features at Lonielist and Cross Lochs, and also in general between the sites. The significant differences in selected vegetation species are consistent with their preferred microhabitats. Both Lonielist and Cross Lochs show a greater proportion of heather (*C vulgaris*) on the higher areas of ground. Cross Lochs has higher percentages of *S capillifolium*, a *Sphagnum* species well known to be hummock forming (Laine, 2009) on the higher areas, and more deer grass (*T germanicum*) in the hollows, whilst Lonielist has significantly more red-stemmed feather moss (*P Schreberi*) in the furrows. It is worth noting that there is ecological succession in play as well as microtopographical features when we consider these three sites, as shown in Hancock *et al.* (2018). The presence of deer grass (*T germanicum*) seems to be associated more with the near-natural site at Cross Lochs, whilst Talaheel has higher relative proportions of common cotton grass (*E angustifolium*) which has been found to colonise disturbed areas of ground (Phillips, 1954).

Malhotra *et al.* (2016) similarly found that there was there was a clear relationship between microtopography and species distribution at the Mer Bleue bog in Canada, and that fine spatial structures explained up to 40% of species distribution.

The selected vegetation species showed some influence on GPP, although this varied between the sites. The two wetter sites, Cross Lochs and Talaheel, showed greater connections between GPP and measures of moisture, both NDWI and soil moisture measured using the probe. Both Lonielist and Cross Lochs showed some correlations between factors linked with microtopography and GPP, although the relationship was stronger at Lonielist. Malhotra et al. (2016) found that water table depth was a significant factor in maintaining distinct vegetation communities on microtopographical features. Their work was done on the Mer Bleue bog in Canada, which can be described as near-natural, and therefore is most similar to our site at Cross Lochs which also had links between microtopography and soil moisture, as shown by the EFA.

The underestimation of the model at high GPP values evident in Figure 4 is likely due to the temperature component of the TG model. Although the temperature component functions partly as a proxy for PAR (as shown by the EFA), the relationship between these two factors is not always linear, and this relationship may be even less strong in maritime temperate climates, where warm but cloudy days occur in summer, and cold but clear days in winter. It is worth noting that the presence of vegetation and water bodies can impact the LST (Solangi, Siyal and Siyal, 2019). The values used in the temperature scaling equation may also be affecting the relationship between the model and actual GPP values. These values were estimated visually by plotting EC values against MODIS LST (see Lees, Quaife, *et al.*, 2019), and may not be completely accurate, particularly at the higher end of the temperature range where we had very little data available.

There was a clear difference between the GPP values from the chambers and the EC towers, with the EC data giving higher results at all three sites (Figure 5). There are many possible reasons for this, including errors from the chamber methodology. The collar insertion method, which involved cutting into the peat and root mass around the collar base, could have damaged the vegetation and so reduced chamber fluxes. Heinemeyer et al. (2011) found that collar insertion prior to using a flux chamber could reduce respiration at peatland sites by up to 30-50%, even several months after insertion. The chamber measurements were also subject to a reduction in PAR, which would have resulted in a small reduction measured relative to actual GPP. Background concentrations of CO_2 within the chambers were monitored to ensure they were close to atmospheric levels at the start of each measurement, and as the measurements were only five minutes long CO_2 build-up is unlikely to have affected the results. Some of the chamber data showed noise, suggesting that there were minor leaks where the chamber was not perfectly sealed. The data from these measurements was still useable but may show slightly lower results than the actual flux. It is possible that there were some changes in chamber volume throughout the experimental period due to collar settling and vegetation growth which were not accounted for in the measurements and could have led to slight under or overestimation (Morton and Heinemeyer, 2018).

Factors affecting the EC fluxes may also be responsible for the differences seen. Cross Lochs, which shows a large difference between EC and chamber GPP results, has an open path sensor compared to the other two sites which have closed paths, and this may have led to inaccuracies in the flux measurements as measurements were only taken during (heavy) rain-free periods and so the gap filling has a degree of bias. (Helbig *et al.,* 2016). The ecosystem respiration results are similar from the chambers and the EC tower (not shown), suggesting that the difference is not caused by the partitioning equations used in EC data processing.

Laine *et al.* (2006) compared NEE from EC and chamber measurements at a blanket bog site in Glencar, Ireland, which is climatically and structurally similar to the Forsinard Flows reserve, and found a correlation of 0.82 between EC and interpolated chamber NEE, even when footprint size and direction variation was not accounted for. They did note, however, that agreement decreased towards the extremes of the temperature range, agreeing with the current work where differences were particularly noticeable in the hotter measurement period in July. Griffis, Rouse and Waddington (2000) also compared chamber and EC fluxes, at a subarctic fen in Manitoba. They found that chamber measurements of GPP were 32% lower than EC GPP results, similar to the current work. They also showed that hummocks dominated the CO_2 fluxes, which corresponds with the Lonielist site showing greater agreement between hummock and EC GPP than between hollow and EC GPP. Similarly, Heikkinen *et al.* (2002) found that carbon fluxes from chamber measurements were somewhat lower than those from EC at a subarctic fen in Northern Finland.

Application of the TG model with MODIS data and small-scale 'm' parameter (TG3) matched chamber data better than hourly EC data, suggesting that the difference between chamber and EC GPP is not only a result of spatial scale. The TG model is clearly very dependent on calibration to measured data, and therefore the uncertainty of measurements used in the model calibration will form a large part of the uncertainty estimates of the TG model.

Generally, the agreement between the TG model and the measured fluxes is shown to be good at small scale (TG1), with correlations of 0.57 to 0.71. The Lonielist and Cross Lochs sites show slightly better agreement than the Talaheel site. Talaheel was also the only site to show almost no connection between microtopography and GPP. This may be due to the recent landscaping of the site to put peat dams in the remaining planting furrows, which has created large flat areas and deep pools, rather than the more natural small hummocks and hollows. It may be the case that the

514 vegetation species have not had time since the work done in 2015/16 to develop their ecological
515 niches. It is also clear that the water levels at Talaheel have been increased by the recent plough
516 furrow blocking, and areas which we would consider hollows are often flooded and so unsuitable
517 for taking flux or spectral measurements. This may also be affecting the agreement with the model,
518 as the Talaheel site might be responding to temperature and seasonal changes differently to sites
519 which have had less recent disturbance.

520 The GPP calculated with the TG model that used data from MODIS (TG2) was strongly correlated
521 with the GPP derived from EC data (correlations of 0.76 to 0.86). This was in agreement with the
522 work done on developing the model in Lees, Quaife, *et al.* (2019). The 'm' parameter calibrated
523 for the TG model against EC data in this study, which uses data from 2017, is higher than that
524 calculated in Lees, Quaife, *et al.* (2019) which used 2015/16 data. This may be because the growing
525 season of 2017 was particularly wet; this supports the development of the annual Temperature,
526 Greenness and Wetness (TGWa) model (Lees, Quaife, *et al.*, 2019), which associates high summer
527 wetness with increased annual GPP (this model was not used in this study as it is designed to give
528 a single annual estimate of GPP, and is therefore not applicable on timescales of less than a year).
529 The entirety of the available data were used for optimising the parameterisation in this model, but
530 this does not cause a type 1 error for two reasons: firstly, the 'm' parameter does not affect
531 correlation, but only estimate size. Secondly, the error size is only considered in relation to the
532 difference between chamber and EC calibration, and therefore we are not testing the accuracy of
533 the model, but whether the calibration method affects the results.

534 Several previous studies suggest that vegetation indices using finer resolution remote sensing data
535 match EC measurements of GPP better than coarser resolution data across a variety of ecosystems
536 (Fu *et al.*, 2014; Knox *et al.*, 2017; Gonzalez del Castillo *et al.*, 2018). Becker *et al.* (2008) found

that hummocks in an oligotrophic pine fen had higher GPP than lawns, and that the percentage cover of hummocks was overestimated when lower resolution imagery was used, resulting in an overestimate of CO_2 uptake. Gatis *et al.* (2017), however, showed that chamber measurements of GPP had strong correlations with vegetation indices calculated from both small-scale camera data and large-scale MODIS data in an upland peatland environment. Similarly, we have found that both small-scale spectrometer data and large-scale MODIS data can be used to give good estimates of GPP in peatland landscapes, but the results are dependent on the calibration. The results of the large-scale TG model using MODIS data gave an average estimate of GPP for the site based on NDVI and LST, and which is not dependent on microfeature classifications. Finer resolution satellites such as Sentinel-2 were not used in this study due to their lack of temperature data meaning that they could not be used to calculate the TG model, but this may become possible in future. Future work should also consider aerial remote sensing as an intermediate scale between field spectrometry and satellite data; data from sensors mounted on both aeroplanes (Carless *et al.*, 2019; Räsänen *et al.*, 2019) and Unmanned Aerial Vehicles (UAVs) (Beyer *et al.*, 2019; Scholefield *et al.*, 2019) have begun to be used to assess peatland condition and vegetation communities, and have the potential to be included in methods to estimate carbon fluxes.

5 Conclusions

In this study we have used a Temperature and Greenness (TG) model to estimate GPP from remotely sensed data at small-scale and large-scale, and compared this to chamber and EC measures of GPP.

The TG model successfully incorporates the factors which have the greatest relationship with GPP at our study sites as shown by the exploratory factor analysis, and so produces an estimate of GPP

559 that correlates with measured GPP at both small and large scales. Our results suggest that the
560 differences in GPP caused by peatland small-scale heterogeneity are temporally and spatially
561 inconsistent at our study sites, and that the TG model provides an average estimate. Future
562 iterations of the TG model should consider investigating the link between PAR and temperature
563 in more detail, and its effects on the model output, as it is hypothesised that this aspect of the model
564 may cause the underestimation of higher GPP values.

565 The EC results for GPP are larger than those from the chambers, possibly due to several reasons
566 including variation within the tower footprint, and the challenges of collar insertion and chamber
567 methodology. The TG model, however, shows good agreement with the chamber data at small-
568 scale and the EC data at large scale, suggesting that the model design is robust at all scales,
569 although dependent on the calibration data used. The authors can therefore recommend the use of
570 the TG model as a powerful tool for estimating peatland GPP across large areas, but reliable local
571 ground measurements should be used for calibration in order to give accurate values.

572

573 *Conflicts of Interest*

574 The authors declare no conflict of interest.

575 *Acknowledgments*

576 Thanks are due to the RSPB for their work on this project, and for site access and access to
577 facilities. Thanks also to the Environmental Research Institute (ERI) for their role in restoration
578 monitoring at the Forsinard Flows RSPB reserve. Thanks to Graham Hambley, Matthew Saunders,
579 Roxane Andersen and Neil Cowie for site set up and work coordination, and Rebecca McKenzie
580 and Peter Gilbert for site maintenance. Thanks to Kevin White and Suvarna Punalekar for
581 spectroradiometer training. Thanks to Alison Wilkinson for making 48 collars for the fieldwork.

582 We are very grateful for the help of our field assistants Ainoa Pravia, Jose van Paassen, Paul
583 Gaffney, Wouter Konings, Elias Costa, Zsofi Csillag, Valeria Mazzola, David and Parissa
584 Lumsden, and Joe Croft.

585 *Funding*

Kirsten Lees was part funded by a studentship from The James Hutton Institute, and part funded by the Natural Environment Research Council (NERC) SCENARIO DTP (Grant number: NE/L002566/1). Tristan Quaife was funded by the NERC National Centre for Earth Observation (NCEO). Myroslava Khomik and Rebekka Artz were funded by The Scottish Government Strategic Research Programme 2016-2021. Jonathan Ritson was funded by the Engineering and Physical Sciences Research Council Twenty-65 project [Grant number EP/ N010124/1]. Much of the restoration work reported in this study was funded by EU LIFE, Peatland Action, HLF, and the RSPB

References

Arroyo-Mora, J. *et al.* (2018) 'Airborne Hyperspectral Evaluation of Maximum Gross Photosynthesis, Gravimetric Water Content, and CO2 Uptake Efficiency of the Mer Bleue Ombrotrophic Peatland', *Remote Sensing*. Multidisciplinary Digital Publishing Institute, 10(4), p. 565. doi: 10.3390/rs10040565.

Becker, T. *et al.* (2008) 'Do we miss the hot spots? – The use of very high resolution aerial photographs to quantify carbon fluxes in peatlands', *Biogeosciences*. European Geosciences Union, 5(5), pp. 1387–1393. doi: 10.5194/bg-5-1387-2008.

Belyea, L. R. and Clymo, R. S. (2001) 'Feedback control of the rate of peat formation', 268(1473), pp. 1315–1321. doi: 10.1098/rspb.2001.1665.

Beyer, F. *et al.* (2019) 'Multisensor data to derive peatland vegetation communities using a fixed-wing unmanned aerial vehicle', *International Journal of Remote Sensing*. Taylor and Francis Ltd., 40(24), pp. 9103–9125. doi: 10.1080/01431161.2019.1580825.

Campbell Scientific (2016) 'INSTRUCTION MANUAL EASYFLUX DL CR3000OP For CR3000 and Open-Path Eddy-Covariance System Revision: 3/18'. Available at: www.campbellsci.com. (Accessed: 9 July 2020).

Carless, D. *et al.* (2019) 'Mapping landscape-scale peatland degradation using airborne lidar and multispectral data', *Landscape Ecology*. Springer Netherlands, 34(6), pp. 1329–1345. doi: 10.1007/s10980-019-00844-5.

Chapman, S. J. *et al.* (2009) 'Carbon stocks in Scottish peatlands', *Soil Use and Management*. Wiley/Blackwell (10.1111), 25(2), pp. 105–112. doi: 10.1111/j.1475-2743.2009.00219.x.

Le Clec'h, S. *et al.* (2018) 'Mapping ecosystem services at the regional scale: the validity of an upscaling approach', *International Journal of Geographical Information Science*. Taylor & Francis, 32(8), pp. 1593–1610. doi: 10.1080/13658816.2018.1445256.

Clement, R. J. *et al.* (2009) 'Improved trace gas flux estimation through IRGA sampling optimization', *Agricultural and Forest Meteorology*. Elsevier, 149(3–4), pp. 623–638. doi: 10.1016/J.AGRFORMET.2008.10.008.

Didan, K. (2015) 'MOD13Q1 V006 | LP DAAC :: NASA Land Data Products and Services'. NASA EOSDIS LP DAAC. doi: 10.5067/MODIS/MOD13Q1.006.

Dinsmore, K. J. *et al.* (2009) 'Spatial and temporal variability in CH4 and N2O fluxes from a Scottish ombrotrophic peatland: Implications for modelling and up-scaling', *Soil Biology and Biochemistry*, 41(6), pp. 1315–1323. doi: 10.1016/j.soilbio.2009.03.022.

626 European Commission (2018) *Regulation on land use, land use change and forestry in 2030*
627 *climate and energy framework adopted | Climate Action*. Available at:
628 https://ec.europa.eu/clima/news/regulation-land-use-land-use-change-and-forestry-2030-climate-
629 and-energy-framework-adopted_en (Accessed: 9 July 2018).

630 Fratini, G. and Mauder, M. (2014) 'Towards a consistent eddy-covariance processing: an
631 intercomparison of EddyPro and TK3', *Atmospheric Measurement Techniques*. Copernicus
632 GmbH, 7(7), pp. 2273–2281. doi: 10.5194/amt-7-2273-2014.

633 Fu, D. *et al.* (2014) 'Estimating landscape net ecosystem exchange at high spatial–temporal
634 resolution based on Landsat data, an improved upscaling model framework, and eddy covariance
635 flux measurements', *Remote Sensing of Environment*. Elsevier, 141, pp. 90–104. doi:
636 10.1016/J.RSE.2013.10.029.

637 Gatis, N. *et al.* (2017) 'Evaluating MODIS vegetation products using digital images for
638 quantifying local peatland CO_2 gas fluxes', *Remote Sensing in Ecology and Conservation*.
639 Edited by N. Pettorelli and M. Disney. Wiley-Blackwell, 3(4), pp. 217–231. doi:
640 10.1002/rse2.45.

641 Gonzalez del Castillo, E. *et al.* (2018) 'Integrating proximal broad-band vegetation indices and
642 carbon fluxes to model gross primary productivity in a tropical dry forest', *Environmental*
643 *Research Letters*. IOP Publishing, 13(6), p. 065017. doi: 10.1088/1748-9326/aac3f0.

644 Griffis, T. J., Rouse, W. R. and Waddington, J. M. (2000) 'Scaling net ecosystem CO2 exchange
645 from the community to landscape-level at a subarctic fen', *Global Change Biology*. John Wiley
646 & Sons, Ltd, 6(4), pp. 459–473. doi: 10.1046/j.1365-2486.2000.00330.x.

647 Hambley, G. (2016) *The effect of forest-to-bog restoration on net ecosystem exchange in The*
648 *Flow Country peatlands.* University of St Andrews.

649 Hambley, G. *et al.* (2019) 'Net ecosystem exchange from two formerly afforested peatlands
650 undergoing restoration in the Flow Country of Northern Scotland.', *Mires and Peat*, 23, pp. 1–
651 14.

652 Hancock, M. H. *et al.* (2018) 'Vegetation response to restoration management of a blanket bog
653 damaged by drainage and afforestation', *Applied Vegetation Science*. Edited by V. Vandvik.
654 Wiley/Blackwell (10.1111), 21(2), pp. 167–178. doi: 10.1111/avsc.12367.

655 Heikkinen, J. E. P. *et al.* (2002) 'Carbon dioxide and methane dynamics in a sub-Arctic peatland
656 in northern Finland', *Polar Research*. Routledge, 21(1), pp. 49–62. doi:
657 10.3402/polar.v21i1.6473.

658 Heinemeyer, A. *et al.* (2011) 'Soil respiration: implications of the plant-soil continuum and
659 respiration chamber collar-insertion depth on measurement and modelling of soil CO2 efflux
660 rates in three ecosystems', *European Journal of Soil Science*, 62(1), pp. 82–94. doi:
661 10.1111/j.1365-2389.2010.01331.x.

662 Helbig, M. *et al.* (2016) 'Addressing a systematic bias in carbon dioxide flux measurements with
663 the EC150 and the IRGASON open-path gas analyzers', *Agricultural and Forest Meteorology*.
664 Elsevier, 228–229, pp. 349–359. doi: 10.1016/J.AGRFORMET.2016.07.018.

665 IUCN (2016) *A Secure Peatland Future A vision and strategy for the protection, restoration and*
666 *sustainable management of UK peatlands*. Available at: http://www.iucn-uk-

667 peatlandprogramme.org/sites/www.iucn-uk-peatlandprogramme.org/files/CONSULTATION
668 DRAFT A Secure Peatland Future_WEB.pdf (Accessed: 9 July 2018).

669 JNCC (2011) *Towards an assessment of the state of UK peatlands*. Available at:
670 http://jncc.defra.gov.uk/pdf/jncc445_web.pdf (Accessed: 3 August 2018).

671 Kljun, N. *et al.* (2015) 'A simple two-dimensional parameterisation for Flux Footprint Prediction
672 (FFP)', *Geosci. Model Dev*, 8, pp. 3695–3713. doi: 10.5194/gmd-8-3695-2015.

673 Knox, S. H. *et al.* (2017) 'Using digital camera and Landsat imagery with eddy covariance data
674 to model gross primary production in restored wetlands', *Agricultural and Forest Meteorology*.
675 Elsevier, 237–238, pp. 233–245. doi: 10.1016/J.AGRFORMET.2017.02.020.

676 Kross, A., Seaquist, J. W. and Roulet, N. T. (2016) 'Light use efficiency of peatlands: Variability
677 and suitability for modeling ecosystem production', *Remote Sensing of Environment*. Elsevier,
678 183, pp. 239–249. doi: 10.1016/J.RSE.2016.05.004.

679 Laine, A. *et al.* (2006) 'Estimating net ecosystem exchange in a patterned ecosystem: Example
680 from blanket bog', *Agricultural and Forest Meteorology*. Elsevier, 138(1–4), pp. 231–243. doi:
681 10.1016/J.AGRFORMET.2006.05.005.

682 Laine, J. (2009) *The intricate beauty of Sphagnum mosses : a Finnish guide for identification*.
683 Department of Forest Ecology, University of Helsinki. Available at:
684 https://portals.iucn.org/library/node/29078 (Accessed: 13 August 2018).

685 Lees, K. J. *et al.* (2018) 'Potential for using remote sensing to estimate carbon fluxes across
686 northern peatlands – A review', *Science of The Total Environment*. Elsevier, 615, pp. 857–874.
687 doi: 10.1016/J.SCITOTENV.2017.09.103.

688 Lees, K.J., Quaife, T., *et al.* (2019) 'A model of gross primary productivity based on satellite
689 data suggests formerly afforested peatlands undergoing restoration regain full photosynthesis
690 capacity after five to ten years', *Journal of Environmental Management*. Academic Press, 246,
691 pp. 594–604. doi: 10.1016/J.JENVMAN.2019.03.040.

692 Lees, Kirsten J. *et al.* (2019) 'Changes in carbon flux and spectral reflectance of *Sphagnum*
693 mosses as a result of simulated drought', *Ecohydrology*. John Wiley & Sons, Ltd. doi:
694 10.1002/eco.2123.

695 Lees, K.J., Clark, J. M., *et al.* (2019) 'Peatland vegetation: field and laboratory measurements of
696 carbon dioxide fluxes and spectral reflectance'. NERC Environmental Information Data Centre.
697 Available at: https://catalogue.ceh.ac.uk/documents/ab9f47f9-9faf-4403-a57e-25e31f581ed0.

698 Levy, P. E. and Gray, A. (2015) 'Greenhouse gas balance of a semi-natural peatbog in northern
699 Scotland', *Environmental Research Letters*. IOP Publishing, 10(9), p. 094019. doi:
700 10.1088/1748-9326/10/9/094019.

701 LI-COR Biosciences (2017) 'Eddy Covariance Processing Software (Version 7.0.6)'. Available
702 at: www.licor.com/EddyPro.

703 Lindsay, R. (2010) *Peatbogs and Carbon: A critical synthesis*. Available at:
704 http://ww2.rspb.org.uk/Images/Peatbogs_and_carbon_tcm9-255200.pdf (Accessed: 9 July 2018).

705 Lindsay, R. A. *et al.* (1988) *The Flow Country - The peatlands of Caithness and Sutherland*.
706 Available at: http://www.jncc.gov.uk/page-4281 (Accessed: 19 October 2018).

Malhotra, A. *et al.* (2016) 'Ecohydrological feedbacks in peatlands: an empirical test of the relationship among vegetation, microtopography and water table', *Ecohydrology*. Wiley-Blackwell, 9(7), pp. 1346–1357. doi: 10.1002/eco.1731.

Met Office (2012) 'Met Office Integrated Data Archive System (MIDAS) Land and Marine Surface Stations Data (1853-current).' NCAS British Atmospheric Data Centre. Available at: NCAS British Atmospheric Data Centre.

Met Office (2018) *Altnaharra SAWS climate information - Met Office*. Available at: https://www.metoffice.gov.uk/public/weather/climate/gfkgdgj2j (Accessed: 9 July 2018).

Moore, D. J. P. *et al.* (2013) 'Persistent reduced ecosystem respiration after insect disturbance in high elevation forests', *Ecology Letters*. Edited by J. Penuelas. Wiley/Blackwell (10.1111), 16(6), pp. 731–737. doi: 10.1111/ele.12097.

Morton, P. A. and Heinemeyer, A. (2018) 'Vegetation matters: Correcting chamber carbon flux measurements using plant volumes', *Science of The Total Environment*. Elsevier, 639, pp. 769–772. doi: 10.1016/J.SCITOTENV.2018.05.192.

Peichl, M. *et al.* (2018) 'Peatland vegetation composition and phenology drive the seasonal trajectory of maximum gross primary production', *Scientific Reports*. Nature Publishing Group, 8(1), p. 8012. doi: 10.1038/s41598-018-26147-4.

Phillips, M. E. (1954) 'Eriophorum Angustifolium Roth', *The Journal of Ecology*. British Ecological Society, 42(2), p. 612. doi: 10.2307/2256893.

R Core Team (2017) 'R: A language and environment for statistical computing.' Vienna, Austria.

Räsänen, A. *et al.* (2019) 'Comparing ultra-high spatial resolution remote-sensing methods in mapping peatland vegetation', *Journal of Vegetation Science*. Edited by D. Rocchini. Wiley-Blackwell, 30(5), pp. 1016–1026. doi: 10.1111/jvs.12769.

Santhana Vannan, S. K. *et al.* (2009) 'A Web-Based Subsetting Service for Regional Scale MODIS Land Products', *IEEE Journal of Selected Topics in Applied Earth Observations and Remote Sensing*, 2(4), pp. 319–328. doi: 10.1109/JSTARS.2009.2036585.

Scholefield, P. *et al.* (2019) 'Estimating habitat extent and carbon loss from an eroded northern blanket bog using UAV derived imagery and topography', *Progress in Physical Geography: Earth and Environment*. SAGE Publications Ltd, 43(2), pp. 282–298. doi: 10.1177/0309133319841300.

Sims, D. A. *et al.* (2008) 'A new model of gross primary productivity for North American ecosystems based solely on the enhanced vegetation index and land surface temperature from MODIS', *Remote Sensing of Environment*. Elsevier, 112(4), pp. 1633–1646. doi: 10.1016/J.RSE.2007.08.004.

Solangi, G. S., Siyal, A. A. and Siyal, P. (2019) 'Spatiotemporal Dynamics of Land Surface Temperature and Its Impact on the Vegetation', *Civil Engineering Journal*. Ital Publication, 5(8), pp. 1753–1763. doi: 10.28991/cej-2019-03091368.

Waddington, J. M. and Roulet, N. T. (1996) 'Atmosphere-wetland carbon exchanges: Scale dependency of CO_2 and CH_4 exchange on the developmental topography of a peatland', *Global*

Biogeochemical Cycles. John Wiley & Sons, Ltd, 10(2), pp. 233–245. doi: 10.1029/95GB03871.

Wan, Z., Hook, S. and Hulley, G. (2015) 'MOD11A2 MODIS/Terra Land Surface Temperature/Emissivity 8-Day L3 Global 1km SIN Grid V006'. NASA EOSDIS LP DAAC. doi: 10.5067/MODIS/MOD11A2.006.

Wang, G. *et al.* (2012) 'A three-dimensional gap filling method for large geophysical datasets: Application to global satellite soil moisture observations', *Environmental Modelling & Software*. Elsevier, 30, pp. 139–142. doi: 10.1016/J.ENVSOFT.2011.10.015.

Wu, J. *et al.* (2011) 'Dealing with microtopography of an ombrotrophic bog for simulating ecosystem-level CO2 exchanges', *Ecological Modelling*. Elsevier, 222(4), pp. 1038–1047. doi: 10.1016/J.ECOLMODEL.2010.07.015.

Wutzler, T. *et al.* (2018) 'Basic and extensible post-processing of eddy covariance flux data with REddyProc', *Biogeosciences*, 15(16), pp. 5015–5030. doi: 10.5194/bg-15-5015-2018.

Zhang, N. *et al.* (2007) 'Scaling up ecosystem productivity from patch to landscape: a case study of Changbai Mountain Nature Reserve, China', *Landscape Ecology*. Springer Netherlands, 22(2), pp. 303–315. doi: 10.1007/s10980-006-9027-9.